Histopathological and Ultrastructural Alterations in The Renal Cortex of Albino Mice Foetuses Induced by Beta-Lactam Antibiotic 'Amoxicillin'

Sahar A. Sabry, Heba I. Rashad, Mohamed A. Shahin
Department of Biological and Geological Sciences, Faculty of Education, Ain Shams University
Corresponding author: Sahar A. Sabry, **Mobile:** (+20) 01204427241, **E-Mail:** aharsabry84@yahoo.com

ABSTRACT

Background: The aim of this investigation was to evaluate the effect of a low and high doses (205 & 820mg/kg body weight, respectively) of the beta-lactam antibiotic amoxicillin on the kidney of maternally treated mice foetuses.

Material and Methods: Pregnant mice were allocated into three groups; the first group served as control (injected with the drug solvent) and those of the other two groups were injected intraperitoneally with two doses (205 & 820 mg/kg body weight) of amoxicillin for 8 days from day 7 till day14 during gestation.

Results: The histological examination of the renal cortex of maternally treated foetuses showed erosion of the parietal cells of Bowman's capsule, hypoplasia of the mesangial cells of the glomerulus, and erosion of the epithelial cells lining the proximal and distal convoluted tubules. At the electron microscopical level, the alternations of the renal cortex of foetuses maternally treated with amoxicillin were represented by, fusion of the foot processes of the podocytes and partial destruction of the apical brush borders microvilli of the proximal convoluted tubule cells. Also, degeneration of some mitochondria, and fragmentation of the rough endoplasmic reticulum elements of the lining cells of some proximal and distal convoluted tubules were observed.

Conclusions: The uses of amoxicillin should be under restricted precautions specially for the pregnant women to avoid the hazardous impact.

Keywords: Amoxicillin -Kidney - Mice foetuses.

INTRODUCTION

β-Lactams are the oldest and the most class of antibiotics used in the treatment of infections [(1)]. The beta-lactam antibiotics are widely used in Egypt for the treatment of many cases of acute otitis media, respiratory and urinary tract infections, skin infections, salmonella infections, and chlamydia infections. Antibiotics are used in pregnancy for treatment of infections, adding that many pregnant women may administrate antibiotics without doctors' prescription [(2)]. Like most drugs, β-lactam antibiotics cross the human placenta and therefore the foetus is exposed to these molecules [(3)]**.** Amoxicillin is assigned to pregnancy category B by the U.S. Food and Drug Administration (FDA)[(4)].

Despite the beneficial role of this drug, yet large-scale study has shown an association between antibiotic use in the mother and infections in their foetuses. It is quite evident that the effects of such this drug on pregnant women and their foetuses have received diminutive attention[(5)].

Otherwise, male albino rats supplemented with amoxicillin (50mg/kg body weight) for five consecutive days exhibited a significant increase in serum AST, ALT, and creatinine levels. These biochemical data were supported by the adverse histopathological observations on the liver and kidney [(6)].

Keeping in mind that amoxicillin is among these drugs which are handled and prescribed during gestation in Egypt; therefore, the aim of the current investigation was to evaluate the histopathological changes of a low and high doses (205&820mg/kg body weight, respectively) of amoxicillin on the renal cortex of maternally treated mice foetuses.

MATERIAL AND METHODS

Dosages and route of administration of the drug

Two doses of amoxicillin were used in the present investigation; 205 and 820mg /kg body weight and were considered as the low and high doses, respectively, and were calculated based on body surface area according to the conversion table recommended by **Reagan-Shaw *et al.*** [(7)]**.** The chosen dosages were nearly comparable to the human effective low and high therapeutic doses [(8)]**.**

Experimental animals

The present investigation is carried out on mature albino mice of pure CD-1 strain with an average body weight of 20-30g obtained from the breeding unit of Theodor Bilharz Research Institute (TBRI), Imbaba, Giza, A.R. Egypt. The experiments were performed parallel to the ethical standards and according to the International Guides for the Care and Use of Laboratory Animals. Pregnancy was achieved by housing one adult virgin female with one well-marked fertile male overnight, from 5 pm until 9 am of the next

Received:27 /7 /2020
Accepted:26 /8 /2020

day. Successful mating was indicated either by the presence of the vaginal plug or by the presence of sperms in the vaginal smears [9]. Females which give positive vaginal smears are considered pregnant and the day of detection was defined as the first day of gestation.

Experimental design

The present investigation was carried out on 24 pregnant mice which were being divided into three groups (8 mice each). The mice were placed in separate cages labeled according to the group they belonged to. The first group is considered as the control group (C) injected intraperitoneally with 0.1 ml physiological saline solution (the solvent of the drug) daily for 8 days during pregnancy from day 7 till day 14 of gestation. The other two groups (A&B) are the drug-treated groups were intraperitoneally injected with amoxicillin (205& 820mg/kg body weight) for 8 days during pregnancy from day 7 till day 14 of gestation, respectively. Pregnant mice of both control and experimental groups were sacrificed on day 19 of pregnancy. They were dissected and their uteri were removed, placed in normal saline solution and the foetuses were taken out.

Histological preparations

For the histological and histopathological examinations, small pieces of the kidney of the control and maternally treated foetuses were removed, fixed in 10% formalin and aqueous Bouin fixatives. Serial transverse sections of 5 µm thick were prepared for hematoxylin and eosin staining, dehydrated, cleared in xylol and mounted by DPX. Stained sections of kidney of control and maternally treated foetuses were examined by light microscope and photomicrographs were made as requested.

Electron microscopic preparations

For ultrastructural evaluation by transmission electron microscopy, freshly excised kidney tissues of control and maternally treated groups were cut into small pieces and fixed directly in cold 4FIG (i.e., 4%formalin+1%glutaraldehyde adjusted at pH 2.2) for 24 hours. Tissue samples were then post-fixed in 1% osmium tetroxide in 0.1 M phosphate buffer (pH7.3), dehydrated in graded ethanolic series, culminating in 100%acetone, and infiltrated with epoxide resin. After polymerization overnight at 60°C, semi-thin sections (0.5µm) were cut, stained with 1% toluidine blue in sodium borate and examined with a light microscope. Areas of renal tissues were selected, and blocks were trimmed accordingly. Ultrathin sections were cut, mounted on 200 mesh copper grids, and stained with uranyl acetate and lead citrate [10]. The stained grids were examined and photographed by a JEOL-JEM-1400EX-transmission electron microscope, at the Regional Center for Mycology and Biotechnology, Al-Azhar University.

Ethical approval:

This study was conducted in accordance with ethical procedures and policies approved by Animal Care and Use Committee of Faculty of science, Ain Shams University, Cairo, Egypt.

RESULTS

A-Histology of the kidney of the control mice foetuses

The kidney of 19-days old control mice foetus is differentiated into two regions: an outer cortex and an inner medulla. It is encapsulated by a thin connective tissue layer, the renal capsule (Fig. 1). The cortical tissue consists of Malpighian corpuscles and renal convoluted tubules. The Malpighian corpuscle is formed of the Bowman's capsule and glomerulus.

The Bowman's capsule consists of two layers of simple squamous epithelium, an outer parietal layer and an inner visceral one, which are separated by a capsular space, the urinary space. The glomerulus is composed of tortuous capillary loops of the afferent and efferent arterioles, supported by the mesangial cells (Figs. 1&2).

The proximal convoluted tubules appear rounded or oval in cross section of the kidney. Each tubule is lined with a single layer of short columnar epithelial cells with indistinct cell boundaries. Their granular cytoplasm stained deeply with eosin and possesses rounded basal nuclei. The free ends of these cells, near the lumen, are provided with a peculiar brush border.

The distal convoluted tubules are lined with cuboidal epithelial cells that possess distinct cell boundaries and contain spherical centrally located nuclei. The cytoplasm of these cells stained less intensely than those of the proximal convoluted tubules. The lumen of the distal convoluted tubule is wider compared with that of the proximal convoluted tubule. (Figs. 1&2). The medulla is composed of the descending and ascending limbs of Henle and the collecting tubules.

B- Histopathological observations

I-Foetal kidney of mice maternally treated with the low dose of amoxicillin

The kidney of 19-days old foetuses maternally treated with 205mg/kg body weight of amoxicillin showed alternations in the renal cortical tissues. These changes included the Malpighian corpuscles and the renal tubules. Atrophy of renal corpuscles and a decrease in glomerular cellularity were observed. The mesangial cells of the glomerulus showed symptoms of hypoplasia that allow conspicuous dilating of the urinary spaces (Figs. 3 – 5). Erosion of the parietal epithelial cells of Bowman's capsule is also reported in these figures. The lining epithelial cells of some proximal and distal convoluted tubules revealed marked coagulative necrosis and their nuclei manifested symptoms of karyolysis as seen in figures (3-5).

Also, the lumina of some proximal convoluted tubules were occluded with hyaline casts as illustrated in figures (4 and 5). In addition, inter-tubular haemorrhagic oedema was also observed (Fig. 3).

Π-Foetal kidney of mice maternally treated with the high dose of amoxicillin

The kidney of 19-days old foetuses maternally treated with 820mg/kg body weight of amoxicillin showed severe histopathological changes in the renal cortical tissues. These alternations included Bowman's capsule and the tubular and intertubular components of the renal cortex.

The hypotrophy of glomerular tufts is observed in figures 6 & 7 and is marked by the decrease in glomerular cellularity (hypocellularity). The glomeruli were shrunk and so the urinary space of Bowman's capsule appeared rather more widened compared with control specimens (Figs 6 – 8). Furthermore, close inspection of these figures illustrated marked erosion of the lining epithelium of the parietal layer of Bowman's capsule.

The most prominent changes that observed in the renal tubules were represented by coagulative necrosis in the cytoplasm of the lining epithelial cells of the proximal and distal convoluted tubules. The nuclei of some affected cells revealed obvious signs of karyolysis (Figs. 6 – 8).

C- Ultrastructural examination of the kidney of control mice foetuses

The ultrastructure observations revealed that each Malpighian corpuscle is formed of the cup-shaped Bowman's capsule and coiled anastomosing blood capillaries, the glomerulus. The Bowman's capsule consists of two layers separated by the urinary space, an outer parietal layer and an inner visceral one. The parietal layer is composed of simple squamous epithelium while the visceral layer is formed of modified epithelial cells, the podocytes. Each podocyte has several processes known as "pedicles". These processes rest upon the basement membrane of the glomerulus leaving narrow slits between them called infiltration slits (Fig.9).

The glomerular capillaries have certain supporting cells adhering to their walls, known as mesangial cells. These cells are separated from the endothelial cells by an amorphous mesangial matrix.

The luminal surface of the proximal convoluted tubules possesses well-developed microvilli which form the so-called brush border. Endocytic vesicles and lysosomes are observed in the apical cytoplasm beneath the microvilli. Numerous elongated or spherical mitochondria are also observed distributed all over the cytoplasm. The nuclei of these cells are relatively large, mostly euchromatic with well-defined nucleoli and distinct nuclear envelopes. They are located at the basal portions of the cells. The basal membrane is regular and of normal thickness (Figs. 10-12).

The distal convoluted tubules are lined by cuboidal epithelial cells. The cells do not have a brush border and instead, they show short scanty microvilli at the apical membrane. The mitochondria are elongated and occupy the cytoplasmic compartment between the basal infoldings. The nuclei are relatively large and their heterochromatin appears adherent to the inner surface of the nuclear envelope (Fig.13). Basement membrane with normal thickness is also observed in the same figure.

D-Ultrastructural examination of the renal cortex of maternally treated mice foetuses

I-Renal cortex of foetuses maternally treated with the low dose of amoxicillin

The electron micrographs of sections of the renal cortex of foetuses maternally treated with the low dose of amoxicillin showed alterations of the renal cortical cells represented by thickening of the Bowman's capsule. The foot processes of podocytes were frequently fused, thus obliterating the infiltration slits (Fig.14). The same figure exhibited the podocytes nuclei with the clumping heterochromatin material.

The examination of the proximal convoluted tubules showed obvious changes in their ultrastructural configuration. The microvilli constituting the brush border of the lining cells were disorganized and partially degenerated. Aggregations of many vesicles and large vacuoles near the basal part of the microvilli were also observed. The mitochondria were swollen, and their matrices were condensed so that their fine structure became obscure. The nuclei showed an irregular nuclear envelope (Figs. 15&16).

Examination of the cells lining the distal convoluted tubules showed partial loss of the basal membrane infoldings. The cytoplasm appeared to be rarified and had disintegrated mitochondria. These mitochondria lost their matrices so that they did not show any demarcation of their detailed fine structures. The affected cells in distal convoluted tubules exhibited nuclei with irregular outlines. The nuclear envelope of such nuclei appeared with dilated nuclear pores and an increase in the heterochromatin content (Fig.17).

Π- Renal cortex of mice foetuses maternally treated with the high dose of amoxicillin

Electron micrographs of sections of the renal cortex of foetuses maternally treated with the high dose of amoxicillin exhibited different alternations in renal cortical tissues. These alternations included thickening of the Bowman's capsule and some alternations in the visceral epithelial cells (the podocytes) of the capsule. The foot processes of the podocytes were frequently fused, thus obliterating the infiltration slit (Fig.18). The nuclei of affected podocytes showed clumps of marginated heterochromatin. Other podocytes appeared shrunken with the small nucleus, obvious margination of the nuclear chromatin and rupture nuclear envelope.

The proximal convoluted tubules showed disrupted microvilli with aggregation of many vesicles and large vacuoles near the basal part of the microvilli. Most mitochondria appeared nearly normal as compared with the control specimens (Figs.19&20). Figure (19) exhibited that the basal part of the proximal tubular cell possessed thickened basement membrane.

It is worthy of mention that electron microscopic examination of a section of renal cortical cells of foetuses maternally treated with the high dose of amoxicillin displayed multinucleated epithelial cells in the renal tubules (Figs. 21&22). The nuclei of these cells were morphologically like the nuclei of normal appearing uninuclear renal tubular cells, as shown in figure (21). The multinucleated cell in this figure possessed elongated oval nuclei with normal morphology. Although the syncytial mass of a degenerated cell was absent, fragmented rough endoplasmic reticulum and few degenerated mitochondria were observed.

On the other hand, a multinucleated giant cell was observed in figure (22). Examination of this figure revealed that the cytoplasm of this cell contained multiple nuclei of various contours and irregular shapes, with occasional one or two prominent nucleoli. Scattered mitochondria, which lost their cristae and small condensed nucleus, with a dense peripheral rim of chromatin were also identified within this cell (Fig. 22).

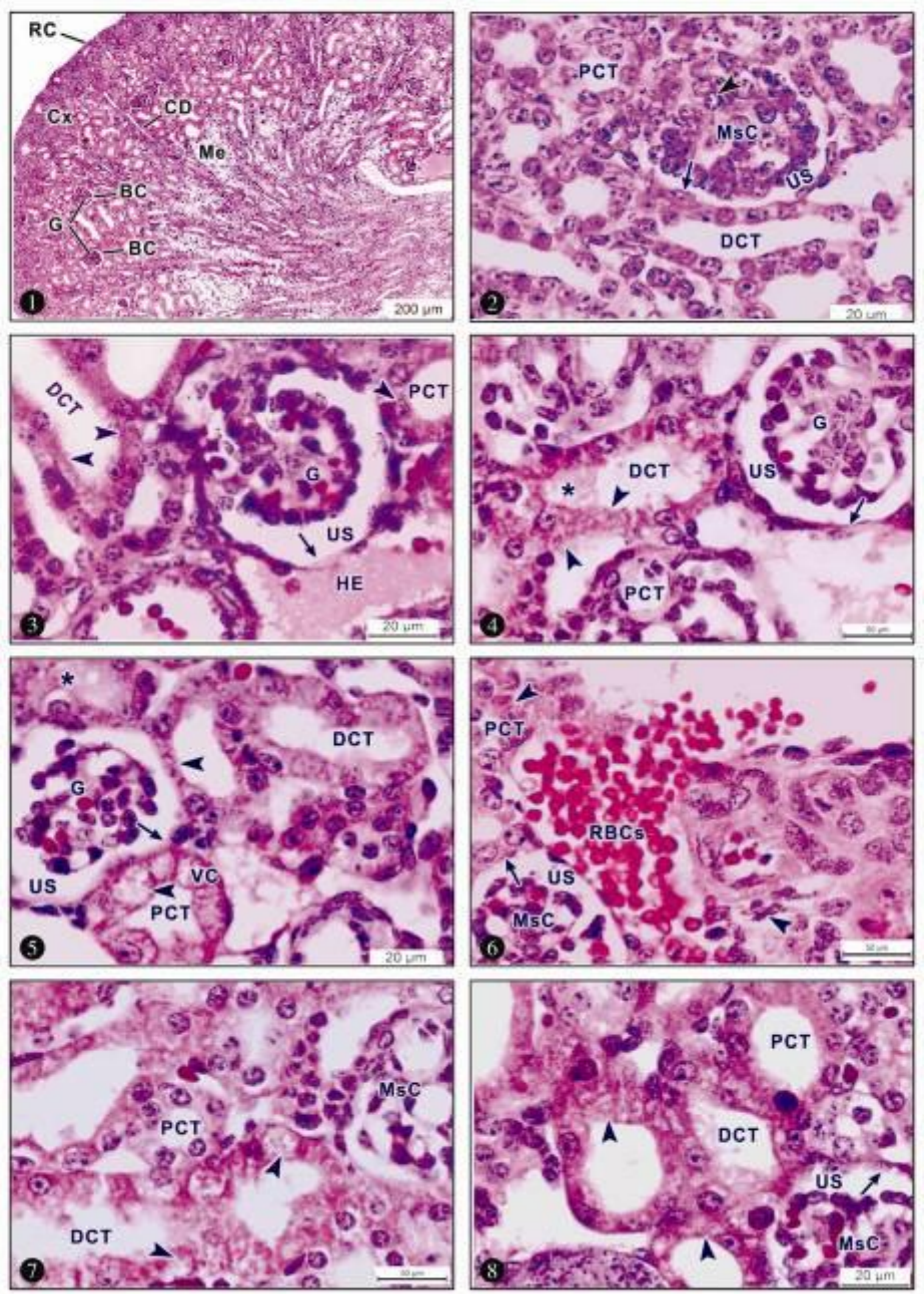
RC
Cx
CD
Me
BC
G
BC
1
200 µm
PCT
MsC
US
DCT
2
20 µm
DCT
PCT
G
US
HE
3
20 µm
G
DCT
*
US
PCT
4
*
DCT
G
US
VC
PCT
5
20 µm
PCT
RBCs
US
MsC
6
MsC
PCT
DCT
7
PCT
DCT
US
MsC
8
20 µm

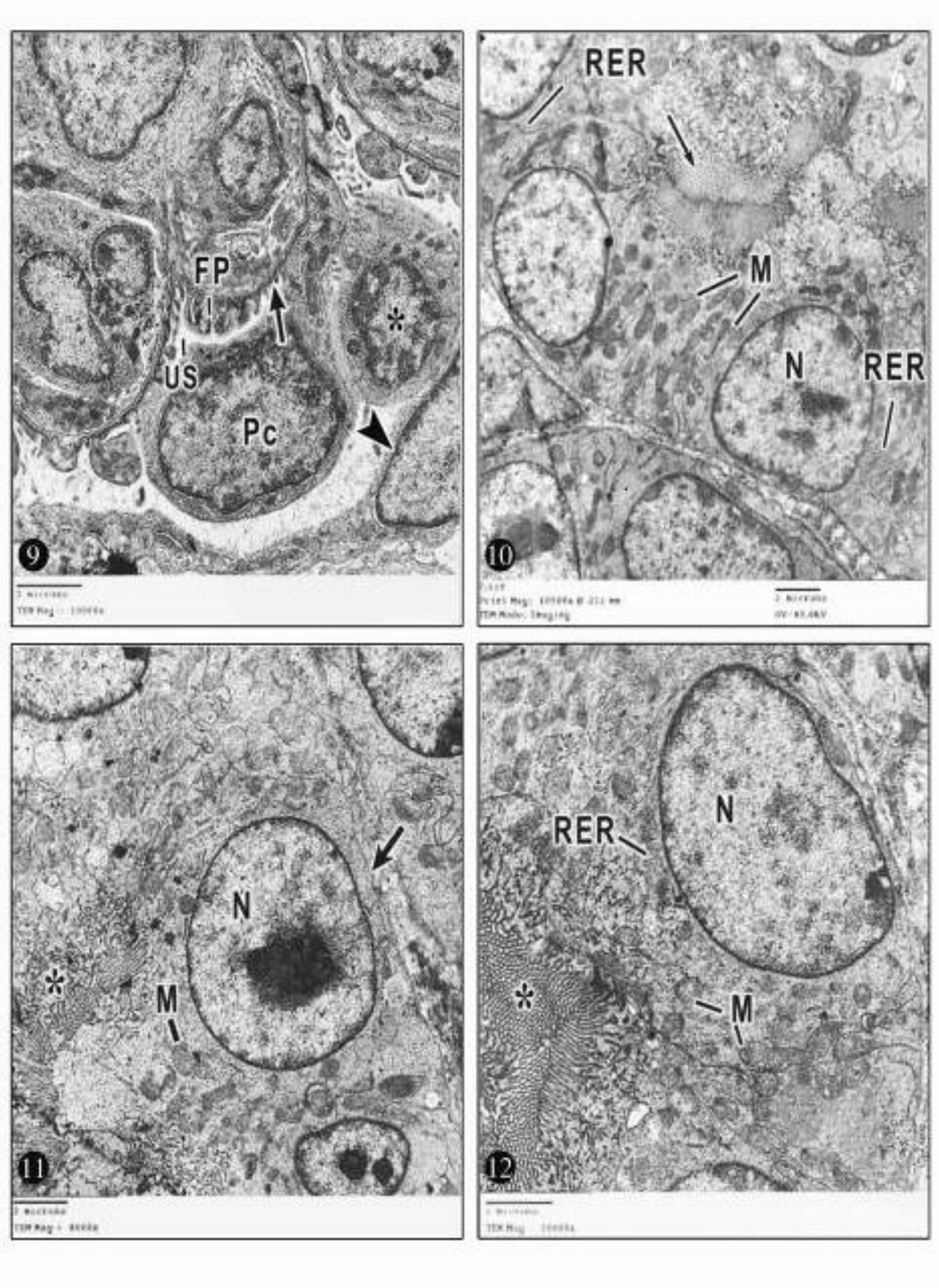
FP
US
Pc
9
RER
M
N
RER
10
N
M
11
RER
N
M
12

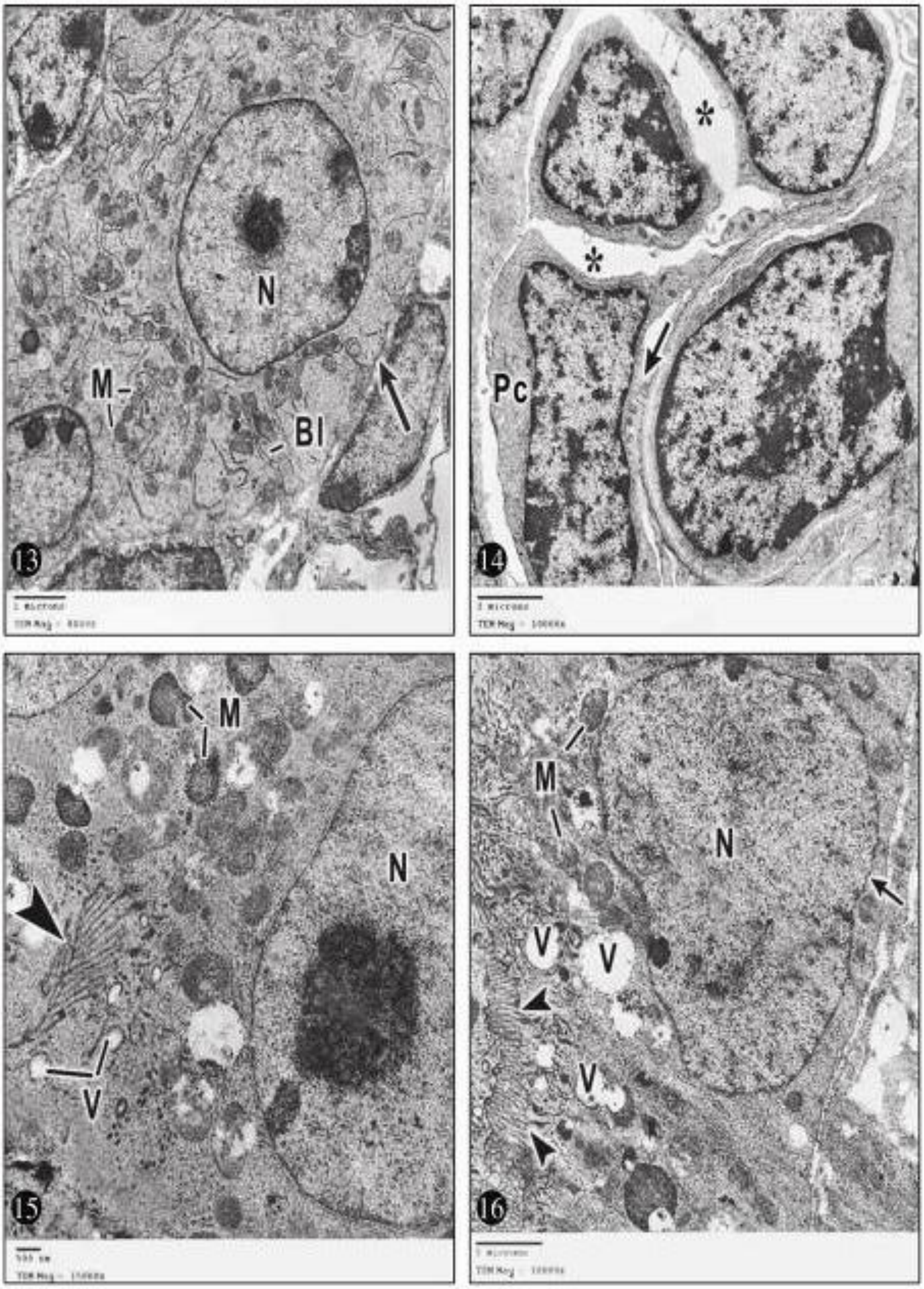
13
N
M
Bl
14
Pc
15
N
M
V
16
N
M
V

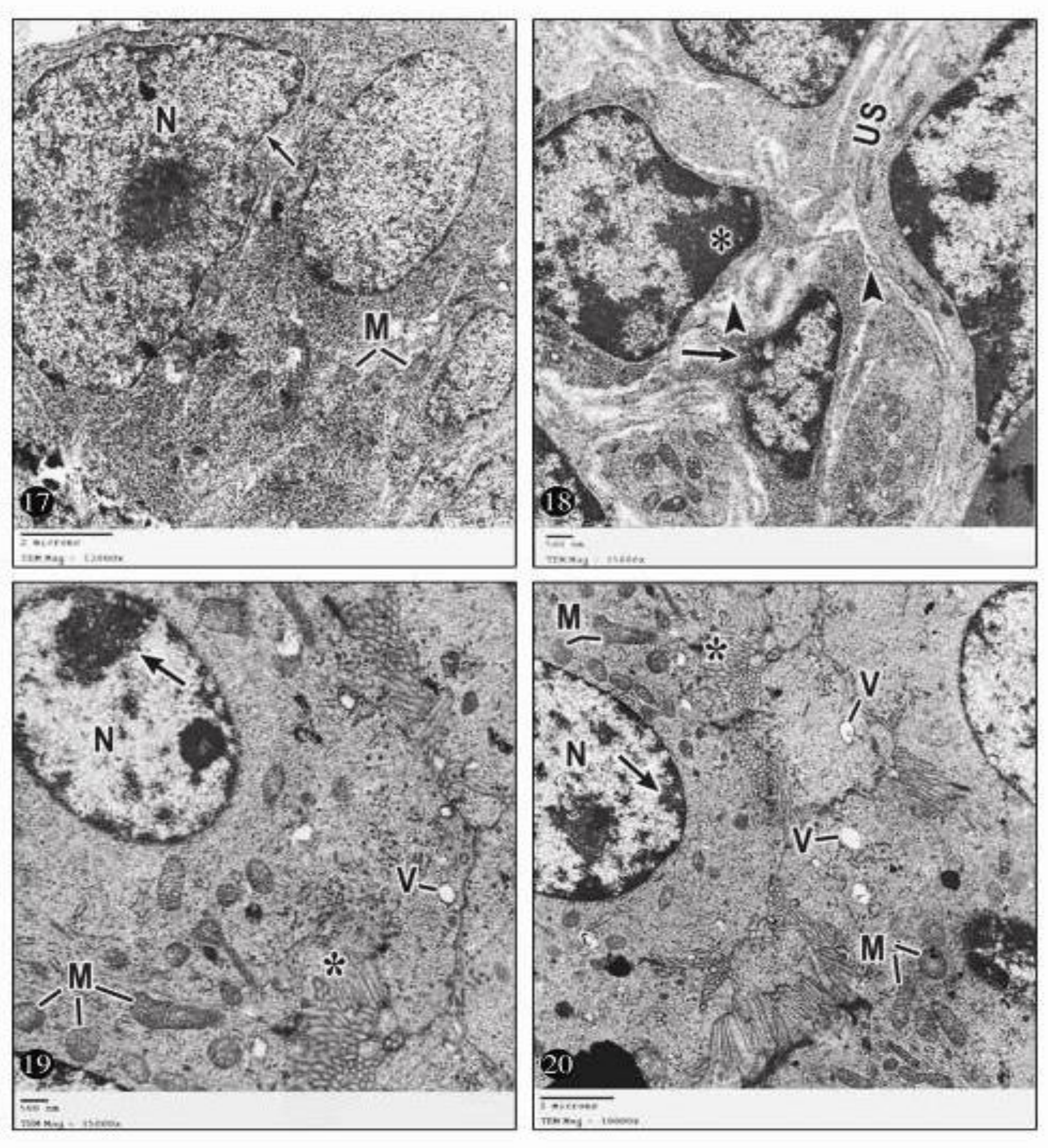
N
M
17
US
18
N
V
M
19
M
N
V
V
M
20

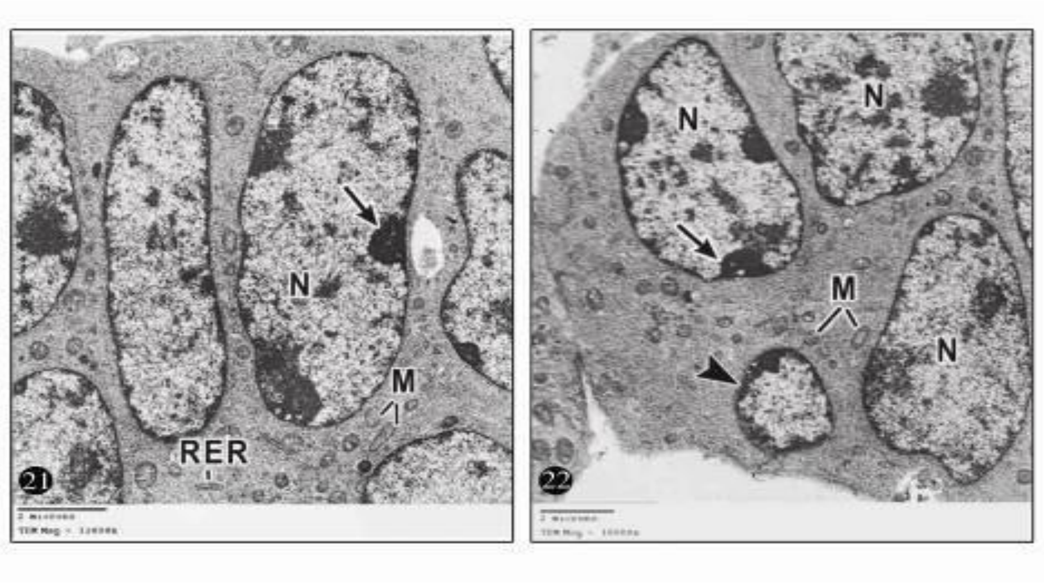
N
M
RER
21
N
N
M
N
22

EXPLANATION OF FIGURES

Figures 1&2: Photomicrographs of kidney sections of 19-days old control mouse foetus stained with H & E.

Fig.1: Showing the two regions of the kidney; the cortex (Cx) and the medulla (Me). The renal capsule (RC), Bowman's capsules (BC), the glomeruli (G) and the collecting ducts (CD) are also noted.

Fig. 2: Showing the parietal epithelial cells of the Bowman's capsule (arrow), the mesangial cells (MsC) of the glomerulus (arrowhead) and the urinary space (US). Several profiles of the proximal (PCT) and distal (DCT) convoluted tubules are also seen.

Figures 3-5: Photomicrographs of kidney sections of 19-days old foetuses maternally treated with low dose of amoxicillin stained with H & E.

Fig. **3**: Showing atrophy of renal corpuscles and a decrease in glomerular cellularity (G). Marked dilation of the urinary space (US) and erosion of the parietal epithelial cells (arrow) of Bowman's capsule. Coagulative necrosis of the lining epithelial cells of some proximal (PCT) and distal (DCT) convoluted tubules was also noted. The nuclei of these injured cells displayed obvious signs of karyolysis (arrow heads). Notice, the intertubular hemorrhagic edema (HE).

Fig.4: Demonstrating erosion of the parietal epithelial cells of Bowman's capsule (arrow), hypoplasia of the mesangial cells of the glomerular tuft(G), and dilation of the urinary space (US). The lining epithelial cells of both proximal (PCT) and distal (DCT) convoluted tubules manifested coagulative necrosis and karyolitic nuclei (arrowheads). The lumina of some tubules were occluded with hyaline casts (*).

Fig.5: Showing cloudy swelling of the lining epithelial cells of both proximal (PCT) and distal (DCT) convoluted tubules; their nuclei manifested karyolysis (arrowheads). The lumina of some convoluted tubules were occluded with hyaline casts (*). Erosion of the parietal epithelial cells (arrow) of Bowman's capsule, hypoplasia of glomerular tuft (G), dilation of the urinary space (US) was also observed. Notice, vacuolated cytoplasm (VC) of epithelial cells of some proximal convoluted tubules.

Figures 6-8: Photomicrographs of kidney sections of 19-days old foetuses maternally treated with the high dose of amoxicillin stained with H & E.

Fig.6: Displaying erosion of the parietal epithelial cells of Bowman's capsule (arrow), hypocellularity of mesangial cells (MsC) and dilated urinary space (US). The lining epithelial cells of some proximal (PCT) convoluted tubules exhibited cloudy swelling and their nuclei showing karyolysis (arrowheads). Accumulation of red blood cells (RBCs) indicated hemorrhagic edema is also observed.

Fig. 7: Showing severe hypoplasia of mesangial cells (MsC) of the glomerulus, the cytoplasm of the lining epithelial cells of both proximal (PCT) and distal (DCT) convoluted tubules exhibit coagulative necrosis, and their nuclei showed karyolysis (arrowheads).

Fig. 8: Showing that the parietal epithelial cells (arrow) of Bowman's capsule exhibited clear symptoms of degeneration. Mesangial cells of the glomerular tuft (MsC) and dilated urinary space (US) are also observed. The proximal (PCT) and distal (DCT) convoluted tubules showed coagulative necrosis in the cytoplasm of their lining epithelial cells and the nuclei displayed obvious signs of karyolysis (arrow heads).

Figures 9-13: Electron micrographs of renal cortex sections of 19-days old control mouse foetus.

Fig. 9: Showing portion of Bowman's capsule illustrated the parietal epithelium (arrowhead), and the urinary space (US). The visceral epithelium is made up of podocytes (Pc) with extended foot processes (FP). Also note the filtration slits (arrow) and the mesangial cell (*).

Fig.10: Showing part of the proximal convoluted tubule has a lumen occupied by a multitude of densely packed microvilli (arrow). The cytoplasm contains numerous elongated mitochondria (M), few stacks of the rough endoplasmic reticulum (RER) and a relatively large nucleus (N).

Fig.11: Illustrating a magnified proximal convoluted tubule cell with delicate numerous microvilli (*), mitochondria (M), and large vesicular nucleus (N) with the well-defined nucleolus. The basement membrane is regular and of normal thickness (arrow).

Fig.12: Illustrating part of proximal convoluted tubule cell with well-developed microvilli (*), numerous mitochondria (M), rough endoplasmic reticulum (RER) and the large oval nucleus (N).

Fig. 13: Displaying part of distal convoluted tubule cell with basal infoldings (Bl), a large number of mitochondria (M) and large spherical nucleus (N), with normal chromatin distribution. The basement membrane (arrow) is also seen.

Figures 14-17: Electron micrographs of sections of the renal cortex of 19-days old foetuses maternally treated with the low dose of amoxicillin.

Fig. 14: Illustrating part of the glomerulus with widening spaces (*) between podocytes. The

podocytes (Pc) processes are fused with swelling foot processes of the blood capillaries. Destructed foot processes (arrow) on some spaces are seen.

Fig. 15: Showing part of the proximal convoluted tubule cell with disrupted microvilli (arrowhead), devastated mitochondria (M) and numerous vacuoles (V) near the basal part of microvilli. Part of the nucleus (N) is also observed.

Fig.16: Revealing another part of the proximal convoluted tubule cell with disrupted microvilli (arrowheads) and many vacuoles (V); the mitochondria (M) appear condensed and lost their internal ridges. The nucleus (N) is surrounded by an irregular nuclear envelope (arrow).

Fig. 17: Illustrating part of the distal convoluted tubule cells contains devastated mitochondria (M). The nucleus (N) with irregular nuclear envelope (arrow).

Figures 18-22: Electron micrographs of sections of the renal cortex of 19-days old foetuses maternally treated with the high dose of amoxicillin.

Fig. 18: Showing part of the glomerulus with the urinary space (US) and destructed foot processes (arrowheads). The nuclei of podocytes exhibited obvious clumping heterochromatin materials (*). Other podocytes appear shrunken with a small nucleus that possesses a rupture nuclear envelope (arrow).

Fig. 19: An electron micrograph showing one of the epithelial cells of the proximal convoluted tubule. The cell shows degenerated microvilli (*), mitochondria (M), and pinocytotic vacuole (V). The nucleus (N) with clumps of heterochromatin (arrow) is also seen.

Fig.20: Showing proximal convoluted tubule cells with degenerated microvilli (*), numerous mitochondria (M), and pinocytotic vacuoles (V). The nucleus (N) with marginated heterochromatin (arrow) is also observed

Fig. 21: Revealing a portion of the renal tubules displayed a multinucleated epithelial cell with elongated oval nuclei (N), fragmented rough endoplasmic reticulum (RER) and degenerated mitochondria (M). The peripheral rim of chromatin is also noticed in the nuclei (arrow).

Fig. 22: Showing part of the renal tubules exhibited a multinucleated giant cell possessed multiple nuclei (N) of various contours and irregular shapes. Scattered mitochondria (M) and small pyknotic nucleus (arrowhead) with a dense peripheral rim of chromatin (arrow) were also identified.

DISCUSSION

The present histological investigation illustrated variable histopathological alterations in the renal tissues of mice foetuses maternally treated with 205&820 mg/kg body weight of amoxicillin. These histological findings are in agreement with those reported by several investigators.

Cortical thinning and reduced glomeruli were observed in the newborn rats maternally exposed to gentamicin during gestation [11]. In the same line, **Lelievre-Pegorier *et al*.** [12] reported diminished glomerular volume in young pups born to guinea pigs that were treated with gentamicin from days 48 to 54 of gestation. In confirmation of these findings, some authors noticed a reduction of the number of nephrons in pups born to rats exposed to gentamicin during gestation [13&14].

In a communication offered by **Nathanson *et al*.**[15], they observed mild cystic tubule dilation in renal tissue in rat pups born to amoxicillin treated mothers. In addition, they marked that amoxicillin altered renal development *in vitro* metanephros organ culture in a dose-dependent manner. The authors suggested that drugs which are associated with few or no side effects in the adult kidney may exert toxic effects on the developing metanephros at therapeutic doses.

The duration of treatment, in the present investigation, extends from day 7 to day 14 of gestation. This period of pregnancy covering organogenesis and overlapping the first stages of renal development in mice foetuses. In mice, nephrogenesis is reported to start by day 11 of gestation and by 17 and 18 days, the kidney is fully differentiated [16]. At this period drugs are known to have the greatest potential to cause malformations [17]. During kidney development, apoptosis is a normal feature in the nephrogenic zone, reaching up to 3% of cells in rat metanephros [18&19]. Exposure to the antibiotics ampicillin or amoxicillin induced more apoptotic cells in the mesenchymal cells [20&15]. The participation of the mesenchyme in nephrogenesis is consistent with previous reports showing that extensive apoptosis affects the number and structure of nephrons [21,22&15].

The aforementioned explanations support the effects of amoxicillin on the renal tissues of maternally treated foetuses obtained in the present investigation. The defects in early nephrogenesis might be due to intrauterine growth retardation as reported by Gilbert *et al*.[14] , who illustrated that partial ligature of uterine arteries, which retards growth, also causes a decrease in the number of nephrons in rat pups at birth. In addition, Such effect may be due to that the foetal renal tissue is functionally immature enough to excrete the drug metabolites rapidly as adult [23].

The results of the current study regarding the ultrastructural alterations in renal tubular cells of foetuses exposed to amoxicillin showed similarity with those reported by several authors. Various ultrastructural changes were observed in renal cortical cells of newborn rats of mothers subjected to the gentamicin during pregnancy; these alterations include the nuclei and deposits of myelin-like material in the mitochondria [24-26].

In a similar trend, **Pedrycz *et al*.**[27] indicated that administration of the antibiotic adriamycin to mothers during pregnancy caused fusion of the podocytes foot processes and degenerative lesions of the lining epithelial cells of the renal tubules of rat foetuses. In addition, treatment with the aminoglycoside antibiotic tobramycin caused ultrastructural changes in the renal cortex of rats[28]. These changes included degeneration in the epithelial cells of proximal convoluted tubules, increased number of lysosomes, and loss of apical microvilli. In the same direction, rats exposed to ciprofloxacin exhibited thickening of glomerular basement membrane, and devastation in the convoluted tubular cells[29].

It is worthy of mention that electron microscopic examination of a section of renal cortical cells of foetuses maternally treated with the high dose of the antibiotic amoxicillin displayed multinucleated epithelial cells in the renal tubules. The presence of multinucleated cells in the proximal convoluted tubules of human kidneys is attributed to pathological changes in the renal tubules (renal sclerosis) [30&31].

The expression of HSP 70 (a biomarker of oxidation stress) was evaluated in renal cells of rat foetuses maternally exposed to adriamycin prior to pregnancy[32]. The authors reported that the antibiotic adriamycin exhibited high affinity to oxygen which resulted in damage of mitochondria in the tubular cells of the fetal kidney. This explanation showed that in spite of the fact that the exact nephrotoxic mechanism of beta-lactam antibiotics (including amoxicillin) is not yet fully established, it has been suggested that this group of antibiotics induced oxidative stress results in tubular damage[33].

CONCLUSIONS

The uses of amoxicillin should be under restricted precautions specially for the pregnant women to avoid the hazardous impact.

REFERENCES

1. **McNamara P, Stoeckel K, Ziegler W (1982):** Pharmacokinetics of ceftriaxone following intravenous administration of a 3-g dose. Eur. J. Clin. Pharmacol., l22: 71–75.
2. **Alsaleh R, Gari S, Gari M (2019):** The awareness of pregnant patient about effect of antibiotics in pregnancy. J. Microsc. Ultrastruct., 7(2):72-77.
3. **Pacifici G, Nottoli R (1995):** Placental transfer of drugs administered to the mother.Clin. Pharmacokinet., 28: 235–269.
4. **Briggs G, Freeman R, Yaffe S (2005):** Drugs in Pregnancy and Lactation. A Reference Guide to Fetal and Neonatal Risk. Seventh ed, Lippincott Williams & Wilkins, Philadelphia. https://cmc.marmot.org/Record/.b43272368
5. **Britoa L, Garciaa L, Caetano M (2018):** Electrochemical remediation of amoxicillin: Detoxification and reduction of antimicrobial activity. Chem. Biol. Interact, 291: 162–170.
6. **El-Safty Z, El-Sayed M, Elbadawy M (2018):** Hepato-renal adverse effects of amoxicillin and doxycycline in rats. World J. Pharm. Pharm. Sci., 7 (2): 1-12.
7. **Reagan-Shaw S, Nihal M, Ahmad N (2008):** Dose translation from animal to human studies revisited. FASEB J., 22 (3): 659-661.
8. **Kaur S, Rao R, Nanda S (2011):** Amoxicillin: A broad spectrum antibiotic. Int. J. Pharm. Pharm. Sci., 3(3): 30-37.
9. **Snell G (1956):** Biology of The Laboratory Mouse. 5th ed, the Blakiston Company, Philadelphia.
10. **Dykstra M, Mann P, Elwell R *et al.* (2002):** Suggested standard operating procedures (SOPs) for the preparation of electron microscopy samples for toxicology/pathology studies in a GLP environment. Toxicol. Pathol., 30: 735-743.
11. **Mallié J, Gerard H, Gerard A (1986):** In-utero gentamicin-induced nephrotoxicity in rats. Pediatr. Pharmacol. (New York, NY), 5(4): 229-239.
12. **Lelievre P, Gilbert T, Sakly R *et al.* (1987):** Effect of fetal exposure to Gentamicin on kidneys of young guinea pigs. Antimicrob. Agents Chemother, 31 (Pt 1): 88-92.
13. **Mallié J, Gerard H, Gerard A (1984):** Gentamicin administration to pregnant rats. Effect on fetal renal development in utero. Dev. Pharmacol. Ther., 7: 89-92.
14. **Gilbert T, Lelievre-Pegorier M, Malienou R *et al*. (1987):** Effects of prenatal and postnatal exposure to gentamicin on renal differentiation in the rat. Toxicology, 43(3): 301-313.
15. **Nathanson S, Moreau E, Merlet-Benichou C *et al*. (2000):** *In utero* and *in vitro* exposure to β-lactams impair kidney development in the rat. J. Am. Soc. Nephrol., 11(5): 874-884.
16. **Horster M, Braun G, Huber S (1999):** Embryonic renal epithelia: Induction, nephrogenesis and cell differentiation. Physiol. Rev., 79(4):1157-1191.
17. **Vallance P (1996): Drugs and the foetus:** Caution is needed in all women of childbearing age. Br. Med. J., 312: 1053–1054.
18. **Coles H, Burne J, Raff M (1993):** Large-scale normal cell death in the developing rat kidney and its reduction by epidermal growth factor. Development, 118(3): 777-784.
19. **Savill J (1994):** Apoptosis and the kidney. J. Am. Soc. Nephrol., *5*(1): 12-21.

20. **Koseki C, Herzlinger D, Al-Awqati Q (1992):** Apoptosis in metanephric development. J. Cell Biol., 119: 1327–1333.
21. **Veis D, Sorenson C, Shutter J *et al*. (1993):** Bcl-2-deficient mice demonstrate fulminant lymphoid apoptosis, polycystic kidneys, and hypopigmented hair. Cell, 75: 229–240.
22. **Sorenson C, Rogers S, Korsmeyer S *et al*. (1995):** Fulminant metanephric apoptosis and abnormal kidney development in bcl-2-deficient mice. Am. J. Physiol., 268: 73–81.
23. **Guyton A, Hall E (2006):** Textbook of Medical Physiology. Elsevier Saunders, Inc. Library of Congress Cataloging, New York, Pp. 307-325.
24. **Kosek J, Mazze R, Cousins M (1974):** Nephrotoxicity of gentamicin. Lab. Invest., 30: 48-57.
25. **Aubert-Tulkens G, Van Hoof F, Tulkens P (1979):** Gentamicin induced lysosomal phospholipidosis in cultured rat fibroblasts. Lab. Invest., 40: 481-491.
26. **Laurent G, Carlier M, Rollmann B *et al*. (1982):** Mechanism of aminoglycoside-induced lysosomal phospholipidosis: *In vitro* and *in vivo* studies with gentamicin and amikacin. Biochem. Pharmacol., 31: 3861-3870.
27. **Pedrycz A, Boratynski Z, Wieczorski M *et al*. (2005):** Ultrastructural and immunohistochemical evaluation of apoptosis in foetal rat liver after adriamycin administration. Bull. Vet. Inst. Pulawy., 49(4): 475-478.
28. **Al-Motabagani M (2007):** Histological study on the effect of tobramycin dosage regimens on renal proximal tubular cells in the rats. Pak. J. Med. Sci., 23(1): 71-77.
29. **El-Hawwary A, Sarhan N (2017):** Does olive oil attenuate ciprofloxacin-induced renal cortical toxicity? Light and electron microscopic study. Egypt. J. Histol., 40(2): 253-264.
30. **Harman J, Hogan J (1949):** Multinucleated epithelial cells in the tubules of the human kidney. Arch. Pathol., 47: 29-36.
31. **Heptinstall R, Kissane J, McCluskey R *et al.* (1974):** Pathology of the Kidney, 2nd ed, Little Brown and Company, Boston., Pp. 355.
32. **Pedrycz A, Brzeski Z (2006):** L-arginine decreases heat shock protein 70 (marker of environmental stress) expression in kidney cells of rat foetuses during apoptosis-late effect of adriamycin action. Ann. Agric. Environ., Med., 13(1): 129-132.
33. **Pazhayattil G, Shirali A (2014):** Drug-induced impairment of renal function. Int. J. Nephrol. Renovasc. Dis., 7: 457–468.